

## Ultraslow Polaron Dynamics in Low-Doped Manganites from $^{139}\text{La}$ NMR-NQR and Muon Spin Rotation

G. Allodi, M. Cestelli Guidi, and R. De Renzi

*Dipartimento di Fisica e Istituto Nazionale di Fisica della Materia, Università di Parma, I-43100 Parma, Italy*

A. Caneiro

*Centro Atómico Bariloche, San Carlos de Bariloche, Argentina*

L. Pinsard

*Laboratoire de Physico-Chimie des Solides, UMR 8648, Université Paris-Sud, 91405 Orsay Cédex, France*

(Received 29 March 2001; published 30 August 2001)

We report a  $^{139}\text{La}$  NMR investigation of low-doped insulating manganite samples ( $\text{LaMnO}_{3+\delta}$  and  $\text{La}_{1-y}\text{Ca}_y\text{MnO}_{3+\delta}$ ) as a function of temperature. A volume fraction with fast nuclear relaxations was revealed by the inhomogeneous loss of the NMR signal over a broad temperature interval. Comparison with muon spin rotation data demonstrates that the *wipeout* of the  $^{139}\text{La}$  signal is mainly due to slowly fluctuating electric field gradients. This provides strong evidence for the slow diffusion of lattice excitations, identified with Jahn-Teller small polarons.

DOI: 10.1103/PhysRevLett.87.127206

PACS numbers: 75.30.Vn, 71.38.-k, 71.70.Ej, 75.30.Kz

Lanthanum manganites  $\text{La}_{1-x}\text{A}_x\text{MnO}_3$  ( $\text{A} = \text{alkali-earth metal}$ ) have attracted great interest because of their correlated magnetic and transport properties, which include a colossal magnetoresistance (CMR) at suitable composition ( $x \approx 0.3$ ). Recently the role of the electron-lattice coupling has been emphasized. Millis *et al.* [1] pointed out that the metal-insulator transition causing CMR arises from the crossover from a large Jahn-Teller (JT) polaron to a small JT polaron regime. Experimental evidence of the involvement of lattice degrees of freedom in the electronic properties has been provided in recent years by a giant isotopic effect on  $T_c$  and on the EPR linewidth [2], by transport [3,4] and electric thermopower [5] measurements, and by optical spectroscopies [6,7]. The prominent role of the JT effect in manganites is now widely accepted among the physics community. Direct evidence of local lattice distortions, identified with JT polarons, has also been provided by the pair distribution function (PDF) from neutron diffraction data [8,9]. PDF, however, yields only the rms lattice distortion, without any information on lattice dynamics.

This paper addresses the issue of polaron dynamics in low-doped, insulating manganites by means of  $^{139}\text{La}$  NMR and muon spin rotation ( $\mu\text{SR}$ ). We will show that, throughout this region of the phase diagram,  $^{139}\text{La}$  actually probes a slow diffusion of charged entities which are straightforwardly identified with lattice polarons.

The investigated samples were  $\text{LaMnO}_{3+\delta}$  and  $\text{La}_{1-y}\text{Ca}_y\text{MnO}_{3+\delta}$ , with hole concentration  $0 \leq x \leq 0.23$  ( $x = y + 2\delta$ ).  $\text{La}_{0.95}\text{Ca}_{0.05}\text{MnO}_3$  was a twinned single crystal grown by the floating zone method. The other samples were sintered powders prepared by standard solid state reaction. Details of sample preparation and characterization are reported elsewhere [10,11]. Resistivity of the doped samples was measured by the four-lead method. The

most doped sample,  $\text{La}_{0.8}\text{Ca}_{0.2}\text{MnO}_{3.015}$ , exhibits a metallic behavior, with a resistivity maximum near  $T_c = 190\text{ K}$  and  $d\rho/dT > 0$  at  $T < T_c$ , while the other samples are insulators.

$^{139}\text{La}$  NMR was performed in an applied field of 7 T, in a temperature range of 40–360 K. Spectra were recorded point by point with a standard  $90^\circ - \tau - 90^\circ$  spin echo sequence on a phase coherent spectrometer. The pulse delay  $\tau$  was kept as short as possible, limited by the dead time of the receiver following the transmission of a rf pulse (typically 10–14  $\mu\text{s}$ ). At all temperatures the spin-spin relaxation rates  $T_2^{-1}$  were determined by varying  $\tau$ , and the echo amplitude decay was best fitted by two exponentials. The spin echo amplitudes were extrapolated back to  $\tau = 0$ , and divided by the NMR sensitivity  $\propto \omega^2/k_B T$ . With this correction, the integrated amplitudes of each spectrum are proportional to the number of nuclei giving rise to the signal.  $\mu\text{SR}$  spectra were recorded at ISIS (Chilton, UK), on either the MUSR or EMU instruments. The data shown here are part of an extensive  $\mu\text{SR}$  investigation of La manganites, reported elsewhere [12].

$^{139}\text{La}$  NMR is sensitive both to the magnetic and to the electronic structure. Lanthanum nuclei ( $\gamma/2\pi = 6.014\text{ MHz/T}$ ) are coupled to the neighboring Mn electronic spins by a transferred hyperfine interaction. The local field  $\mathbf{B}_l$ , including the external field  $\mu_0\mathbf{H}$ , has the form

$$\mathbf{B}_l \equiv \frac{\omega_L}{\gamma} = \frac{2\pi}{\gamma} g\mu_B \sum_j^{n,n_i} C_j \langle S_j \rangle + \mu_0\mathbf{H}. \quad (1)$$

The hyperfine coupling constant is estimated in all lanthanum manganites as  $C \approx 0.1\text{ T}/\mu_B$  [13–15]. Owing to nearly cubic symmetry of the lanthanum site, the transferred hyperfine field on  $^{139}\text{La}$  is approximately proportional to the ferromagnetic moment of the surrounding

Mn octet. At  $T \ll T_c$ , the spontaneous field ranges from  $\approx 3.5$  T ( $\nu_L \approx 20$  MHz) in a fully ferromagnetic (F) environment [13,14], down to a small but nonzero value of  $\approx 300$  mT in the pure antiferromagnetic (AF) structure of  $\text{LaMnO}_3$  [15], due to the distortion of the perovskite cell. In the paramagnetic (P) phase, large frequency shifts proportional to the magnetic susceptibility are produced by hyperfine couplings in the presence of external field. Note that in the present experiments we do not expect any critical divergence of the nuclear relaxations rates near the magnetic transition, since AF fluctuation modes yield negligible instantaneous fields at the La site, and F fluctuations are suppressed by the intense external field [16].

In addition,  $^{139}\text{La}$  ( $I = 7/2$ ) is coupled to the local electric field gradient (EFG) tensor  $V_{ij}$  through its electric quadrupole moment  $Q$ . In the frame of reference of the EFG principal axes ( $|V_{zz}| \geq |V_{yy}| \geq |V_{xx}|$ ), the nuclear Hamiltonian accounting for both magnetic and electric interactions is written as [17]

$$\mathcal{H}_n = \hbar \gamma \mathbf{B}_l \cdot \mathbf{I} + \frac{h\nu_Q}{6} \left[ 3I_z^2 - I(I+1) + \frac{1}{2} \eta (I_+^2 + I_-^2) \right]. \quad (2)$$

Here  $\nu_Q = 3eQV_{zz}/[2hI(2I-1)]$ , and  $\eta = |V_{xx} - V_{yy}|/V_{zz}$  is the EFG asymmetry parameter. The quadrupole interaction resolves the Zeeman transitions, leading in a single crystal to angle-dependent multilines spectra with quadrupolar satellites. In a polycrystalline sample the angular average of the satellite patterns gives rise to a characteristic powder spectrum.

The spectra of stoichiometric  $\text{LaMnO}_3$  are plotted in Fig. 1a. The spectra fit to quadrupolar powder patterns, broadened by magnetic interactions [18]. The best fit parameters for the EFG are  $\nu_Q = 3.8(1)$  MHz,  $\eta = 0.94(2)$  at all temperatures, in close agreement with data reported by Kumagai *et al.* [15]. The paramagnetic shifts agree with magnetic susceptibility data, which follow a Curie-Weiss law for  $S = 2$ ,  $g = 2$  moments, and the magnetic line broadening is negligibly small at  $T > T_N$ . This indicates a highly homogeneous and accurate stoichiometry for this sample. The onset of an AF order is solely witnessed by a sizable magnetic broadening below  $T_N = 139$  K. Figure 2 shows that the integrated spectral intensity, corrected for the NMR sensitivity, is constant within experimental accuracy, i.e., the signal originates from the whole sample volume at all temperatures.

Spectra from a subset of hole-doped compounds are plotted in Figs. 1b–1d. In the order phase they show magnetic shifts and line broadening increasing at increased doping, in agreement with a ferromagnetic moment increasing with  $x$ . The shifts at 70 K in  $\text{LaMnO}_{3.04}$ ,  $\text{LaMnO}_{3.06}$  (not shown,  $T_c = 125$  and 150 K), and  $\text{La}_{0.87}\text{Ca}_{0.13}\text{MnO}_{3.035}$  ( $T_c = 170$  K) are 7, 12, and 15 MHz, respectively. A comparison with the spontaneous frequency of 20 MHz in the CMR ferromagnet  $\text{La}_{0.7}\text{Ca}_{0.3}-$

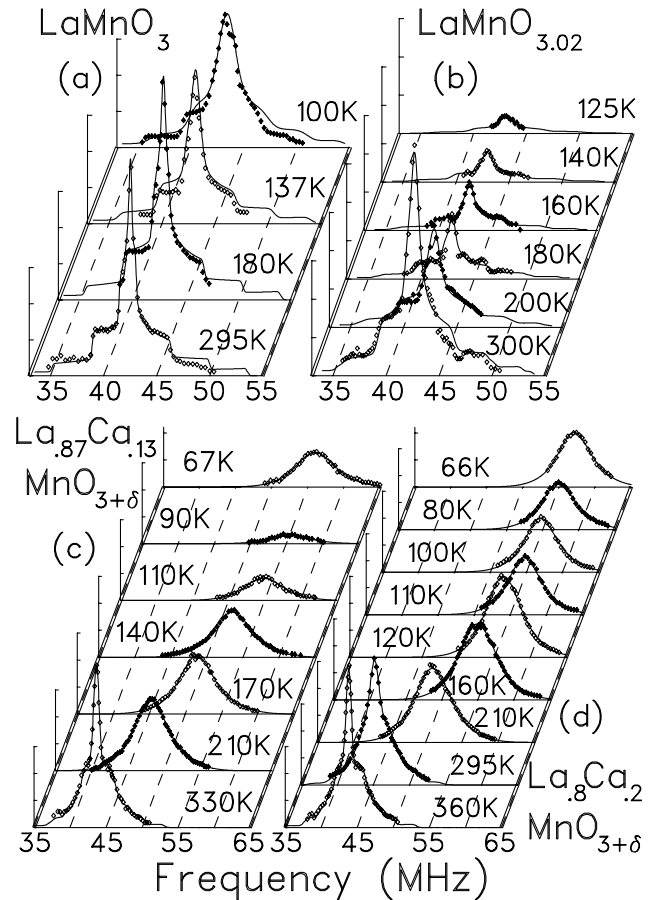


FIG. 1.  $^{139}\text{La}$  NMR spectra in 7 T ( $\gamma\mu_0 H/2\pi = 42.08$  MHz) as a function of temperature from  $\text{LaMnO}_3$  and  $\text{LaMnO}_{3.02}$  (AF),  $\text{La}_{0.87}\text{Ca}_{0.13}\text{MnO}_{3.035}$  (F insulator), and  $\text{La}_{0.8}\text{Ca}_{0.2}\text{MnO}_{3.015}$  (F metal).

$\text{MnO}_3$  indicates  $\approx 35\%$ ,  $60\%$ , and  $75\%$  ferromagnetically polarized Mn octets in the three samples. Furthermore, a dependence of the EFG on composition was observed. In  $\text{LaMnO}_{3.02}$  and  $\text{La}_{0.95}\text{Ca}_{0.05}\text{MnO}_3$  (both  $T_N = 130$  K) the fit yields the same quadrupolar linewidth as in

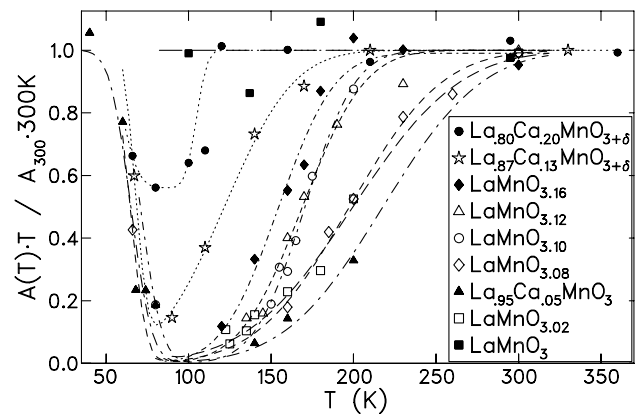


FIG. 2. Relative  $^{139}\text{La}$  NMR integral amplitude from all the samples as a function of temperature. The amplitudes are corrected for  $T_2$ ,  $\nu_L^2$ , and  $T$ . The lines are best fits to the data using the model described in the text.

LaMnO<sub>3</sub> within experimental accuracy. At doping concentrations  $0.06 < x \leq 0.1$ ; however, a progressively reduced EFG was detected, down to  $\nu_Q = 3.0$  MHz,  $\eta = 0.3$  in LaMnO<sub>3.05</sub> ( $T_c = 140$  K), whereas no further EFG reduction was observed in the high temperature spectra at higher doping, up to  $x = 0.23$  in the metallic La<sub>0.8</sub>Ca<sub>0.2</sub>MnO<sub>3.015</sub>. The EFG reduction is probably due to a lower static distortion of the MnO<sub>6</sub> octahedra in the doped compounds.

The most remarkable feature of the La spectra is, however, the strong reduction of the signal amplitude, which occurs over a wide temperature range in all the doped *insulating* samples (Fig. 2). In LaMnO<sub>3.04</sub> ( $T_c = 125$  K) in particular, the signal was completely lost at  $75 \text{ K} \leq T \leq 140$  K. The temperature interval where the signal diminishes depends on composition. It is maximum in the least-doped compounds LaMnO<sub>3.02</sub> and La<sub>0.95</sub>Ca<sub>0.05</sub>MnO<sub>3</sub>, where a missing fraction is already detected at  $T \gg T_c$ , right below room temperature. At increased doping the interval narrows, and its upper limit is lowered down to 140 K in La<sub>0.87</sub>Ca<sub>0.13</sub>MnO<sub>3.035</sub>, a temperature well below  $T_c$ . The full signal amplitude is recovered in all samples only at  $T \leq 60$  K. The missing amplitude in the insulating doped compounds is clearly due to fast and inhomogeneous spin-spin relaxations. This is confirmed by the relaxation time constants  $T_2$  of the measured signals, which actually decrease down to values of order  $10 \mu\text{s}$  as the temperature is lowered, and by echo amplitudes decaying with multiexponential behavior, as shown in Fig. 3. The *wipeout* of the signal originates therefore from a fraction of nuclei with an even shorter  $T_2 \leq 5 \mu\text{s}$ , outside the time window of NMR because of the aforementioned dead time. In the metallic sample La<sub>0.8</sub>Ca<sub>0.2</sub>MnO<sub>3.015</sub>, however, the full signal amplitude is detected at all temperatures, except for a slight amplitude reduction at  $60 \text{ K} < T \leq 110$  K. The small missing fraction in this sample is most likely due to a minority

insulating phase, either due to chemical inhomogeneity or to the electronic phase separation of hole-rich domains. This is also indicated by <sup>139</sup>La nuclear relaxations, which reveal two distinct components (inset of Fig. 3). The minority signal shows larger relaxation rates increasing with decreasing temperature, similar to those of the insulating compounds. The majority component displays the opposite temperature dependence typical of fully metallic manganites near optimum composition for CMR [14,19], and its spin-spin relaxation eventually saturates to the Gaussian behavior due to nuclear moments alone (homonuclear linewidth). We relate therefore the wipeout of the signal to the lightly doped insulating phase in all of our samples.

In principle, the fast nuclear relaxations responsible for the <sup>139</sup>La wipeout might be due either to magnetic or to EFG fluctuations,  $T_{2(\text{La})}^{-1} = T_{2M}^{-1} + T_{2E}^{-1}$ . A clarification is provided by the comparison between NMR and  $\mu\text{SR}$  data. Implanted positive muons ( $S_\mu = 1/2$ ) are another local probe of magnetism, coupled only to the Mn electronic spins and not to the EFG. Spontaneous precession frequencies  $\nu_L^\mu \geq 80$  MHz have been observed in manganites at  $T \ll T_{c,N}$ , regardless of the AF or F order [20,21]. Longitudinal muon relaxations in the *P* phase in a small applied field of 20 G are shown in Fig. 4 for a typical low-doped sample (LaMnO<sub>3.045</sub>,  $T_c \approx 130$  K). Muons exhibit the full initial polarization and comparatively low Lorentzian relaxation rates  $\lambda_\mu$ , never exceeding  $10^5 \text{ s}^{-1}$  down to  $T_c$ . Above  $T = 250$  K the ratio of the La and muon relaxation rates is  $T_{2(\text{La})}^{-1}/\lambda_\mu = 1/5$ , which indicates that  $T_{2M}^{-1}$  is at most one-fifth of the muon rate. This empirical upper limit implies that  $T_{2M} \geq 5/\lambda_\mu \geq 50 \mu\text{s}$ , also close to  $T_c$  where the La signal vanishes. If the La relaxation were dominated by the magnetic channel it would be safely within the time window of NMR, contrary to the experimental evidence. Note that relaxation rates scale as  $T_{2M}^{-1}/\lambda_\mu = 16(\nu_{\text{La}}/\nu_\mu)^2$ , where  $\nu_{\text{La}}$  ( $\nu_\mu$ ) is the

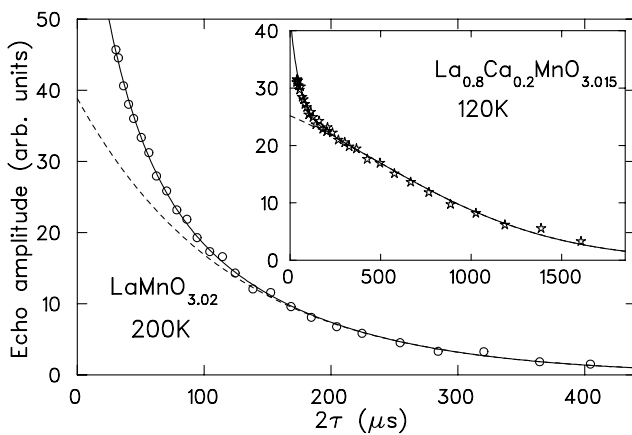


FIG. 3. <sup>139</sup>La transverse depolarization curves ( $T_2$  experiments) for LaMnO<sub>3.02</sub> at 200 K (main figure) and La<sub>0.8</sub>Ca<sub>0.2</sub>MnO<sub>3.015</sub> at 120 K (inset). The decays are best fitted (solid lines) with two time constants; the slower components are marked by the dashed lines.

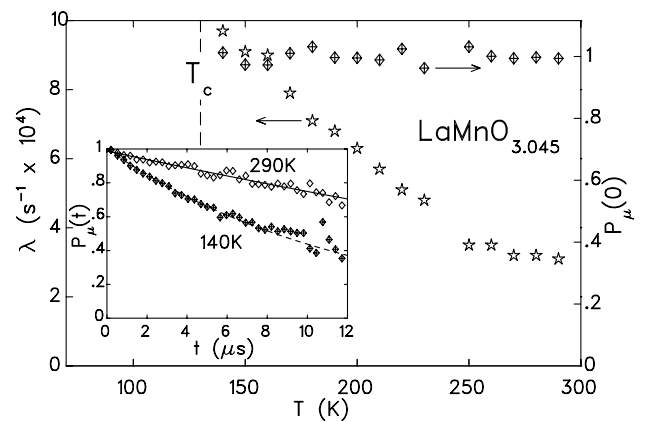


FIG. 4.  $\mu\text{SR}$  of LaMnO<sub>3.045</sub> in a small longitudinal field of 20 G. Main figure: Lorentzian decay rate  $\lambda$  (stars) and initial spin polarization  $P_\mu(0)$  (diamonds) as a function of temperature. Inset: decay of the muon polarization as a function of time  $t$  at two temperatures.

instantaneous frequency in the La ( $\mu$ ) fluctuating hyperfine field [22]. Hence, even in the unrealistic worst case of fully F fluctuations, actually suppressed by the large external magnetic field, the spontaneous precession frequencies in the F state ( $\nu_L^\mu \geq 80$  MHz,  $\nu_L^a \leq 20$  MHz) set a theoretical limit  $T_{2M} \geq \lambda_\mu^{-1} \geq 10 \mu\text{s}$ , still within the time window of NMR. Therefore  $T_{2E}^{-1}$  must dominate in the wiped-out fraction.

A similar loss of the Cu NQR signal intensity was recently reported for the cuprate series  $\text{La}_{2-x-y}\text{R}_y\text{Sr}_x\text{CuO}_4$  ( $R$  = rare earth), which exhibits stripe instability and, close to the concentration  $x = 1/8$ , the localization of static incommensurate charge-ordered stripes below a transition temperature  $T_{\text{charge}}$  [23]. The wipeout of the Cu signal was ascribed to the *glassy* slowing down of the stripes, which are dynamic above  $T_{\text{charge}}$  [24]. In the case of cuprates, however, it is still debated whether the diverging nuclear relaxations mainly involve spin or charge degrees of freedom [25].

In lightly doped manganites no long range superstructure has ever been detected above  $T_c$ . Here, the wipeout of the La signal must arise from the diffusion of short range charge excitations coupled to lattice distortions. A fine dispersion of these centers is actually indicated by the residual NMR signal, which also relaxes very fast and with several time constants, such as in the case of a distribution of distances between the diffusing local distortion and the La nuclei. As in cuprates, however, the diffusion slows down continuously without any critical behavior as the temperature is lowered, as in a glass transition. A relaxation model adapted from Curro *et al.* [25] fits our  $^{139}\text{La}$  amplitude data (Fig. 2); we assume (i) an instantaneous quadrupolar frequency  $\Delta\omega_Q$  fluctuating with a Lorentzian spectrum and a correlation time  $\tau_c = \tau_\infty \exp(E_a/k_B T)$ , (ii) an inhomogeneous  $T_2^{-1} = \Delta\omega^2 \tau_c$  arising from a distribution of either the activation energy  $E_a$  or  $\Delta\omega_Q$ , and (iii) the recovery of the signal in the static limit whereby  $\tau_c$  is longer than the duration  $\Delta t$  of the whole pulse sequence ( $\Delta t \approx 30 \mu\text{s}$ ). The narrowing of the wipeout temperature interval at increasing doping corresponds to the decrease of  $\bar{E}_a/k_B$  from 750(50) K in  $\text{LaMnO}_{3.02}$  down to 350(50) K in  $\text{La}_{0.87}\text{Ca}_{0.13}\text{MnO}_{3.035}$ . Assuming also for convenience EFG fluctuations of comparable amplitude to the static EFG (i.e.,  $\Delta\omega_Q/2\pi \approx 1$  MHz), the following threshold for the occurrence of the wipeout can be established:  $\bar{\tau}_c \geq 10^{-9}$  s. We stress that direct determination of collective dynamics on this time scale is only accessible to slow microscopic probes such as NMR-NQR and  $\mu\text{SR}$ .

It is remarkable that the wipeout occurs throughout the whole *low-doping insulating* region of the phase diagram, whereas it is absent in both the undoped and the metallic phases. This peculiar fact, namely, the occurrence of this phenomenon under the combination of charge carriers and a macroscopic insulating behavior, strongly suggests that the diffusing centers are JT *small polarons*. The recovery of the full signal amplitude at approximately the

same temperature  $T_{\text{rec}} \approx 60$  K in all the samples denotes the freezing of the polarons, which appear static to NMR at  $T < T_{\text{rec}}$ . It is worth noting that, in the same composition range investigated here, Millis [26] recently reported private communications with Cheong on a charge-ordered (CO) phase at low temperature. The flat phase boundary of the CO region with  $T_{\text{CO}}(x) \approx 60\text{--}70$  K is in good agreement with our nearly  $x$ -independent  $T_{\text{rec}}$ . We therefore associate the polaron freezing with the onset of a CO state. If the identification holds, the CO transition may be viewed as the transition from a polaron liquid to a polaron crystal.

In conclusion, comparison of  $^{139}\text{La}$  NMR and  $\mu\text{SR}$  data from low-doped manganites demonstrates the slow diffusion of charge-lattice excitations, which we identify with small JT polarons.

This work was partially supported by a MURST-PRIN 2000 grant "*Polaroni magnetoelastici*." Discussions with G. Guidi and M. Hennion are gratefully acknowledged.

- 
- [1] A. J. Millis *et al.*, Phys. Rev. Lett. **74**, 5144 (1995); A. J. Millis *et al.*, Phys. Rev. Lett. **77**, 175 (1996).
  - [2] Guo-meng Zhao *et al.*, Nature (London) **381**, 676 (1996); A. Shengelaya *et al.*, Phys. Rev. Lett. **77**, 5296 (1996).
  - [3] J. M. De Teresa *et al.*, Phys. Rev. B **54**, 1187 (1996); J. M. De Teresa *et al.*, Nature (London) **386**, 256 (1997).
  - [4] M. Ziese *et al.*, Phys. Rev. B **58**, 11 519 (1998).
  - [5] M. Jaime *et al.*, Phys. Rev. B **54**, 11 914 (1996).
  - [6] K. H. Kim *et al.*, Phys. Rev. Lett. **81**, 1517 (1998).
  - [7] V. Dediu *et al.*, Phys. Rev. Lett. **84**, 4489 (2000).
  - [8] S. J. L. Billinge *et al.*, Phys. Rev. Lett. **77**, 715 (1996).
  - [9] D. Louca *et al.*, Phys. Rev. B **56**, 8475 (1997).
  - [10] F. Prado *et al.*, J. Solid State Chem. **146**, 418 (1999).
  - [11] M. Hennion *et al.*, Phys. Rev. B **56**, 497 (1997).
  - [12] R. De Renzi *et al.*, Physica (Amsterdam) **289B**, 52 (2000); R. De Renzi *et al. ibid.* **289B**, 85 (2000).
  - [13] M. K. Gubkin *et al.*, JETP Lett. **60**, 56 (1994).
  - [14] G. Allodi *et al.*, Phys. Rev. Lett. **81**, 4736 (1998).
  - [15] K. Kumagai *et al.*, Phys. Rev. B **59**, 97 (1999).
  - [16] T. Moriya, Prog. Theor. Phys. **28**, 371 (1962).
  - [17] A. Abragam, *The Principles of Nuclear Magnetism* (Clarendon Press, Oxford, 1961), p. 232.
  - [18] The quadrupole satellites were calculated up to second order in  $\nu_Q/\nu_L$ . Powder average was computed numerically after an algorithm in D. W. Alderman *et al.*, J. Chem. Phys. **84**, 3717 (1986).
  - [19] M. M. Savosta *et al.*, Phys. Rev. B **59**, 8778 (1999).
  - [20] R. J. Heffner *et al.*, Phys. Rev. Lett. **77**, 1869 (1996).
  - [21] M. Cestelli Guidi *et al.*, Phys. Rev. B, (to be published).
  - [22] The numerical prefactor (16) originates from the rate equations for the central  $^{139}\text{La}$  transition [R. R. Ernst, G. Bodenhausen, and A. Wokaun, *Principles of Nuclear Magnetic Resonance in One and Two Dimensions* (Oxford University Press, Oxford, 1987), p. 55].
  - [23] J. M. Tranquada *et al.*, Nature (London) **375**, 561 (1995).
  - [24] A. W. Hunt *et al.*, Phys. Rev. Lett. **82**, 4300 (1999).
  - [25] N. J. Curro *et al.*, Phys. Rev. Lett. **85**, 642 (2000).
  - [26] A. J. Millis, Nature (London) **392**, 147 (1998).